Ab initio CASPT2//CASSCF study of the $O(^1D)+H_2O(X\,^1A_1)$ reaction

R. Sayós,[a] Carolina Oliva, and Miguel González[a]
Departament de Química Física i Centre de Recerca en Química Teòrica, Universitat de Barcelona, C/Martí i Franquès, 1. 08028 Barcelona, Spain

(Received 30 January 2001; accepted 14 August 2001)

The ground potential energy surface (PES) of the $O(^1D)+H_2O$ system was studied with the CASPT2//CASSCF *ab initio* method. We analyzed the degree of validity of an earlier *ab initio* study by us that used the Møller–Plesset (MP) method. Both the present CASPT2//CASSCF calculations and the highest level MP calculations (PUMP4//UMP2) showed that the main reaction channel (OH+OH) has no energy barrier along the minimum energy path. This result is consistent with the absence of experimental activation energy. The CASPT2//CASSCF and PUMP4//UMP2 results, however, show important differences, mainly concerning the energy, due to the dominant open-shell singlet character of the ground PES. To make an accurate general description of this system, *ab initio* calculations using multireference methods like the one discussed here are required. Nevertheless, the earlier PUMP4//UMP2 calculations can be taken as a reasonable starting point for characterizing the ground PES of this system. Moreover, the pseudotriatomic $(O(^1D)+H–(OH))$ analytical potential energy surface derived in the previous work to interpret the experimental results is a reasonable model for describing the $O(^1D)+H_2O\rightarrow 2\,OH$ reaction. [DOI: 10.1063/1.1408298]

I. INTRODUCTION

The reactivity of the oxygen atom in its first excited electronic state, $O(^1D)$, is important in various fields of chemistry. Its reaction with water is relevant in stratospheric chemistry in the context of ozone degradation processes through the OH/HO_2 catalytic cycle.[1,2] The great difference between the reactive behavior of $O(^1D)$ and that of the ground state oxygen atom, $O(^3P)$, is also of general interest.

The aim of this theoretical research was to study the gas phase reactions involved in the $O(^1D)+H_2O$ system, considering the ground potential energy surface (PES):

$$O(^1D)+H_2O(X\,^1A_1)\rightarrow 2\,OH(X\,^2\Pi),\quad \Delta H^\circ_{0K}=-28.9\ \text{kcal mol}^{-1}\ \text{(Ref. 3)} \tag{1}$$

$$\rightarrow H_2(X\,^1\Sigma_g^+)+O_2(a\,^1\Delta g),\quad \Delta H^\circ_{0K}=-24.8\ \text{kcal mol}^{-1}\ \text{(Ref. 3)} \tag{2}$$

$$\rightarrow H(^2S)+HO_2(X\,^2A''),\quad \Delta H^\circ_{0K}=5.6\ \text{kcal mol}^{-1}\ \text{(Ref. 3)}. \tag{3}$$

Reaction (1) is known to be very fast, the thermal rate constant value approaching the gas kinetics value. The recommended rate constant value for reaction (1), $k(1)$, is $2.2\times10^{-10}\,\text{cm}^3\,\text{molecule}^{-1}\,\text{s}^{-1}$ over the temperature range 200–350 K.[4] This suggests that reaction (1) proceeds without activation energy, unlike what happens for the analogous reaction with $O(^3P)$. At 298 K the $k(2)/k(1)$ ratio was found to be 0.01,[5] while there is no information available on reaction (3).

The nascent internal energy distribution of the OH radical has been measured in several experiments using the laser-induced fluorescence (LIF) technique.[6–17] These mainly involved the $^{16}O(^1D)+H_2{}^{18}O\rightarrow{}^{16}OH+{}^{18}OH$ reaction to differentiate between the new and old OH bonds formed. The reaction with D_2O has also been studied in some cases.[9,17] The $O(^1D)$ atom was generated by photodissociation of either N_2O or O_3. Therefore, OH rovibrational, spin–orbit and lambda-doublet populations involving different collision energies were determined. Analogous studies to those reported for reaction (1) were reported for the corresponding photon-initiated half reaction from the $N_2O\cdot H_2O$,[15,17] $N_2O\cdot D_2O$,[17] and $O_3\cdot H_2O$ (Ref. 13) van der Waals complexes ($H_2{}^{18}O$ in Refs. 13 and 15). The stereodynamics of reaction (1) for the state-specific reaction channel leading to $OH(v'=2, N'=5)$ was also examined[16] using polarized Doppler-resolved LIF spectroscopy.

The findings on the internal energy distributions of ^{16}OH and ^{18}OH and their stereodynamics, are explained by considering that reaction (1) takes place mainly through a microscopic mechanism which involves an HOOH collision complex. This complex is formed by insertion of the $O(^1D)$ atom

[a]Authors to whom correspondence should be addressed. Electronic mail: r.sayos@qf.ub.es, miguel@qf.ub.es

into an OH bond of the H_2O molecule. The average lifetime of the collision complex should be of the same order as the HOOH rotational period, and would not allow for complete energy redistribution between the two OH fragments.

Although there are quite a lot of experimental studies reported on reaction (1), the theoretical information available is very limited. Thus, until very recently the theoretical studies were mainly devoted to characterizing the PES around the hydrogen peroxide molecule[18–20] and OH+OH long-range[21] regions. However, in a previous study of our own[22] a Møller–Plesset (MP) *ab initio* characterization of the $O(^1D)+H_2O$ ground PES was performed and a triatomic analytical representation of the surface was derived. This PES was used in a quasiclassical trajectory (QCT) dynamics study of reaction (1). To the best of our knowledge, that contribution is the first *ab initio* study carried out on the ground PES of the $O(^1D)+H_2O$ system including all possible reaction channels, and is also the first theoretical study on the dynamics of reaction (1). In another work[23] we examined the dynamics of reactions (1) and (3) using the above-mentioned PES.

In this paper, reactions (1)–(3) are characterized at a higher *ab initio* level (multi-reference method) than that reported in Ref. 22, to verify the degree of validity of the above-mentioned Møller–Plesset study. Sections II and III of the paper deal with the *ab initio* methods and *ab initio* results, respectively, and the summary and conclusions are given in Sec. IV.

II. *AB INITIO* METHODS

The following PES correlate with the different asymptotic regions of reactions (1)–(3) under C_1 and C_S symmetries: (a) reactants: $5\,^1A(C_1)$ and $3\,^1A'+2\,^1A''(C_S)$; (b) products of reaction (1): $4\,^1A+4\,^3A(C_1)$ and $2\,^1A'+2\,^1A''+2\,^3A'+2\,^3A''(C_S)$; (c) products of reaction (2): $2\,^1A(C_1)$ and $^1A'+{}^1A''(C_S)$; (d) products of reaction (3): $^1A+{}^3A(C_1)$ and $^1A''+{}^3A''(C_S)$. Hence, all asymptotes may correlate adiabatically through a $^1A(C_1)$ or a $^1A''(C_S)$ PES. Although C_1 is the most general symmetry for the dynamics of reactions that involve four or more atoms, Sec. III shows that most of the stationary points located on the ground PES of this system have symmetry higher than C_1.

We carried out an *ab initio* study of the ground PES (^1A) using the MOLCAS 4.1 program.[24] In addition, we performed some intrinsic reaction coordinate (IRC) calculations with the GAMESS 96 program.[25] The wave function associated with this system is mostly multi-referent for the ground PES. Thus, in most of the PES regions the system behaves as an open-shell singlet, and the wave function is single referent only for arrangements close to the geometry of the closed-shell minima min 1 and H_2O_2 (hydrogen peroxide). Hence, the most suitable *ab initio* methods to study this PES are of multireference type, such as the CASSCF (complete active space self-consistent field) and CASPT2 methods. In the CASPT2 method the CASSCF wave function is taken as the zeroth-order function for calculating energy at the second order of perturbation theory.

The calculations were performed at the CASSCF(14,10) *ab initio* level (full valence space), where (14,10) means that the 14 valence electrons are distributed in 10 active orbitals. The CASSCF(14,10) calculations amount to 2528 configuration state functions (CSF) in C_S symmetry (4950 CSF in C_1 symmetry). Calculations performed in C_S symmetry show an active space composed by $(7a',3a'')$ or $(8a',2a'')$ orbitals, depending on the region of the PES. The active space that leads to the lowest CASSCF energy was chosen in all cases. The dynamic correlation was included by employing the G2 variant[26] of the CASPT2 method. Although several correlation-consistent Dunning basis sets were considered, the standard triple zeta one (cc-pVTZ, 88 basis functions for the whole system) was used for most of calculations.

III. *AB INITIO* RESULTS

The results obtained for the H_2O, OH, H_2, $O_2(a\,^1\Delta_g)$, and HO_2 reactant and product molecules and for H_2O_2, using the CASPT2(G2)//CASSCF(14,10)/cc-pVTZ method (namely, optimal geometries are obtained at the CASSCF level and pointwise CASPT2 calculations are performed on the resulting structures), show a good agreement with experimental information and are very similar to our previous Møller–Plesset (MP) results[22] (Table I).

The energy of the three product asymptotes and of the H_2O_2 hydrogen peroxide minimum using different methods and basis sets is shown in Table II. For the CASSCF calculations, the asymptotes are best described with the aug-cc-pVTZ basis set [relative errors of 1.2% and 10.9% for reactions (1) and (2), respectively], except for reaction (3). The best result for this reaction is furnished by the cc-pVTZ basis set (quantitative agreement with experiment). For the CASPT2//CASSCF calculations, the best result is always obtained with the cc-pVQZ basis set. For the three reaction energies the CASSCF method is in better accord with the experiment than the CASPT2//CASSCF one. However, for the H_2O_2 molecule the CASPT2//CASSCF results are closer to the experimental data than the CASSCF ones.

For all systems studied, the 6-311G$(2d,2p)$ basis set led to results quite similar to those derived from the cc-pVTZ one. Moreover, disregarding reaction (3), results of comparable quality to the best ones mentioned above were obtained with the PUMP4(FU)//UMP2(FC) method [namely, spin-projected unrestricted fourth-order Møller–Plesset perturbation theory correlating all electrons (FU) and considering the geometry obtained at the UMP2 frozen-core (FC) level].[22] This corresponds to the highest level Møller–Plesset method employed in Ref. 22. For the H_2O_2 molecule, the 6-311G$(2d,2p)$ basis set led to somewhat better agreement with experiment than the cc-pVTZ one.

In the following, the reported data correspond to the CASPT2(G2)//CASSCF(14,10)/cc-pVTZ level of calculation [the energies are given with respect to reactants, including zero point energy (ZPE), unless otherwise indicated]. The structures [CASSCF(14,10)/cc-pVTZ level] of the stationary points placed between reactants and products are plotted in Figs. 1 (transition states) and 2 (minima). Their energies [CASSCF(14,10)/cc-pVTZ and CASPT2(G2)//CASSCF(14,10)/cc-pVTZ], including the CASSCF(14,10)/

TABLE I. Properties of reactants, products and H_2O_2 molecule.

		This work[a]	Previous work (Ref. 22)[b]	Experimental data[c]
$H_2(X\ ^1\Sigma_g^+)$	R_e/Å	0.7553	0.7363	0.741 44
	D_e/eV	4.602 (4.134)	4.697	4.749
	ω_e/cm^{-1}	4237.00	4521.62	4401.213
$OH(X\ ^2\Pi)$	R_e/Å	0.9742	0.9621	0.969 66
	D_e/eV	4.489 (3.642)	4.629	4.624
	ω_e/cm^{-1}	3661.12	3867.37	3737.76
$O_2(a\ ^1\Delta_g)$	R_e/Å	1.2311	1.2281	1.215 63
	D_e/eV	8.351 (7.393)	8.350	8.160
	ω_e/cm^{-1}	1448.05	1416.93	1483.50
$H_2O(X\ ^1A_1)$	R_{OH}/Å	0.9638	0.9552	0.957 921
	<HOH/°	102.58	104.06	104.4996
	D_e(H–OH)/eV	5.287 (4.666)	5.441	5.440
	ω_i/cm^{-1}	3760.43	3892.26	3650 A_1 (*s*-stretch)
		1708.36	1649.27	1588 A_1 (bend)
		3864.96	3989.72	3742 B_2 (*a*-stretch)
$HO_2(X\ ^2A'')$	R_{OO}/Å	1.3530	1.3080	1.330 51
	R_{OH}/Å	0.9749	0.9667	0.9708
	<OOH/°	103.05	104.77	104.30
	D_e(H–O_2,HO–O)/eV	2.149 (1.734), 2.994 (2.042)	2.135,2.904	2.259, 2.875
	ω_i/cm^{-1}	3604.12	3720.94	3415.1 A' (OH stretch)
		1434.78	1466.54	1397.8 A' (bend)
		1053.41	1243.53	1100.3 A' (OO stretch)
$H_2O_2(X\ ^1A)$	R_{OO}/Å	1.4798	1.4466	1.4556
	R_{OH}/Å	0.9682	0.9600	0.967
	<OOH/°	98.78	99.82	102.32
	<HOOH/°	115.52	112.05	113.70
	D_e(HO–OH,HOO–H)/eV	2.358 (1.803), 3.853 (3.403)	2.411,4.136	2.348, 4.204
	ω_i/cm^{-1}	3722.34	3845.28	3609.8 *A* (OH *s*-stretch)
		1412.60	1438.67	1395.9 *A* (OH *s*-bend)
		838.12	935.42	865.9 *A* (OO stretch)
		330.71	401.19	<400 *A* (Torsion)
		3719.68	3842.29	3610.7 *B* (OH *a*-stretch)
		1300.69	1331.40	1264.6 *B* (OH *a*-bend)

[a]Geometries and frequencies at the CASSCF(14,10)/cc-pVTZ level and dissociation energy at the CASPT2(G2)//CASSCF(14,10)/cc-pVTZ level (the CASSCF(14,10)/cc-pVTZ results are given in parentheses).
[b]Geometries and frequencies at the UMP2(FC)/6-311G($3d2f$,$3p2d$) level and dissociation energy at the PUMP4(FU)//UMP2(FC)/6-311G($3d2f$,$3p2d$) level.
[c]References 27–36.

TABLE II. Energy of products and H_2O_2 using different methods and basis sets.

Method	E + ZPE/kcal mol^{-1} [a,b]			
	$H_2O_2(X\ ^1A)$	$2OH(X\ ^2\Pi)$	$H_2(X\ ^1\Sigma_g^+)+O_2(a\ ^1\Delta_g)$	$H(^2S)+HO_2(X\ ^2A'')$
CASSCF(14,10)/cc-pVTZ	−65.40 (−68.24)	−29.54 (−26.67)	−29.20 (−23.98)	5.60 (10.23)
CASSCF(14,10)/cc-pVQZ	⋯ (−67.68)	−29.29 (−26.42)	−28.20 (−22.96)	6.58 (11.22)
CASSCF(14,10)/aug-cc-pVTZ	−64.53 (−67.40)	−29.25 (−26.39)	−27.50 (−22.30)	6.92 (11.55)
CASSCF(14,10)/6-311G($2d$,$2p$)	−66.55 (−69.45)	−30.86 (−27.96)	−30.42 (−25.12)	4.50 (9.10)
CASPT2(G2)//CASSCF(14,10)/cc-pVTZ	−80.00 (−82.85)	−31.34 (−28.46)	−31.62 (−26.40)	1.37 (6.01)
CASPT2(G2)//CASSCF(14,10)/cc-pVQZ	⋯ (⋯)	−30.47 (−27.60)	−30.21 (−24.98)	2.81 (7.45)
CASPT2(G2)//CASSCF(14,10)/aug-cc-pVTZ	⋯ (⋯)	−31.55 (−28.49)	−30.42 (−25.22)	1.75 (6.38)
CASPT2(G2)//CASSCF(14,10)/6-311G($2d$,$2p$)	−79.24 (−82.15)	−32.68 (−29.78)	−32.35 (−27.06)	0.46 (5.10)
PUMP4(FU)//UMP2(FC)/6-311G($3d2f$,$3p2d$)	−77.45 (−80.68)	−27.65 (−25.08)	−29.99 (−24.85)	10.27 (14.70)
Experimental data[c]	−78.3±0.1	−28.9±0.6	−24.8±0.1	5.6±2.0

[a]Energy referred to reactants. The theoretical values in parentheses correspond to the energy without including the corresponding CASSCF or UMP2 zero point energy.
[b]Absolute values of energy (Hartrees) for $O(^1D)+H_2O$ are −150.836 114 CASSCF(14,10)/cc-pVTZ, −150.849 632 CASSCF(14,10)/cc-pVQZ, −150.840 850 CASSCF(14,10)/aug-cc-pVTZ, −150.822 165 CASSCF(14,10)/6-311G($2d$,$2p$), −151.226 128 CASPT2(G2)//CASSCF(14,10)/cc-pVTZ, −151.311 174 CASPT2(G2)//CASSCF(14,10)/cc-pVQZ, −151.243 233 CASPT2(G2)//CASSCF(14,10)/aug-cc-pVTZ, −151.184 078 CASPT2(G2)//CASSCF(14,10)/6-311G($2d$,$2p$), −151.286 242 PUMP4(FU)//UMP2(FC)/6-311G($3d2f$,$3p2d$).
[c]Reference 3 (ΔH°_{0K}).

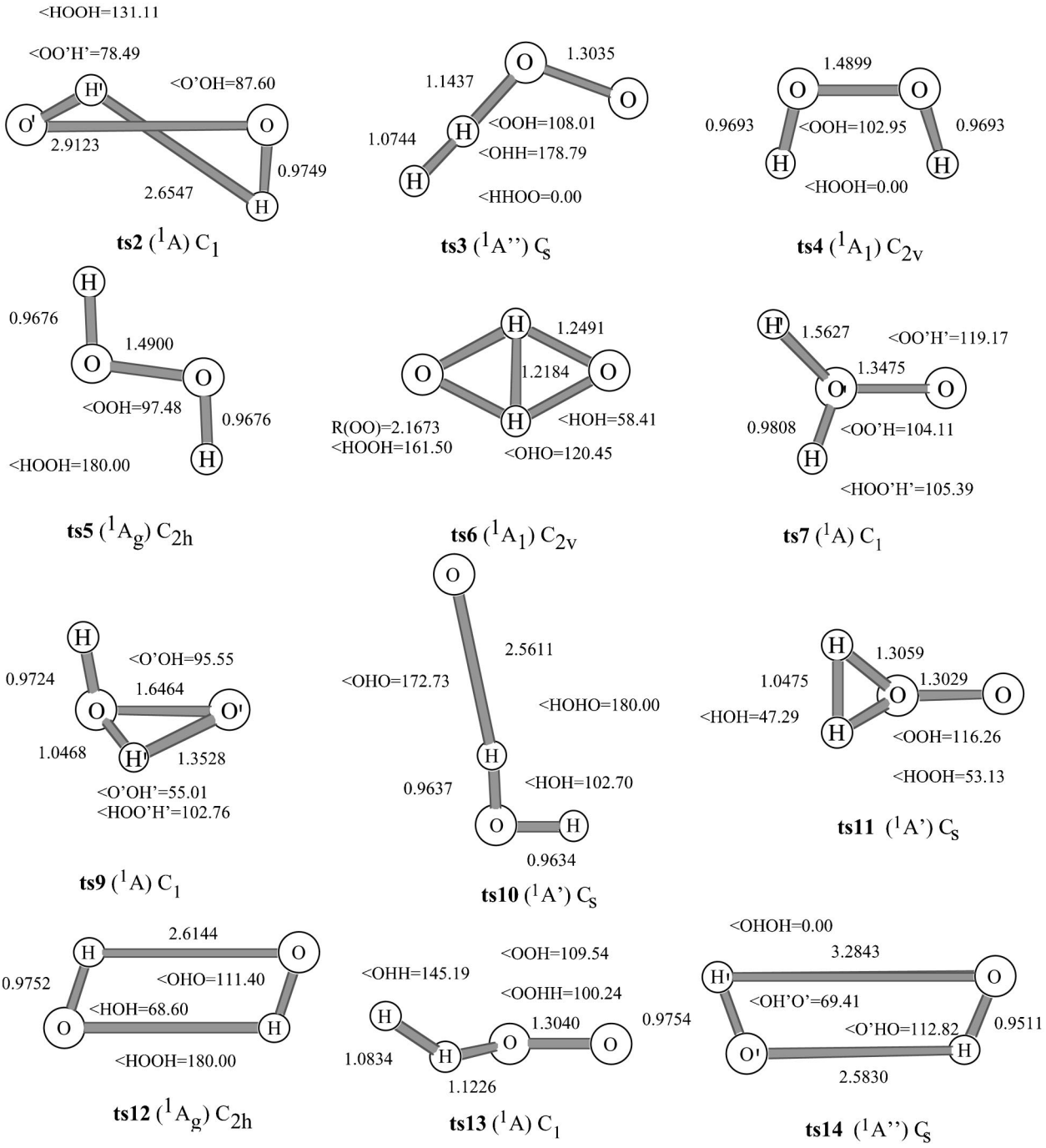

FIG. 1. Transition states of the ground PES at the CASSCF(14,10)/cc-pVTZ level of calculation (ts6 and ts11 are second-order saddle points). Distances are in Angstrom and angles are in degrees.

cc-pVTZ zero point energy, are indicated in Figs. 3 and 4, respectively. In these figures the different reaction pathways for reactions (1)–(3) are also shown schematically, where ''ts'' and ''min'' refer to the transition states (saddle points) and minima, respectively. The harmonic vibrational frequencies [CASSCF(14,10)/cc-pVTZ] of the stationary points are reported in Table III. The electronic structure of the ground PES can be described qualitatively in terms of the dominant electronic configurations of the stationary points found. This information is given in Table IV.

Reaction (1) can occur through two possible reaction pathways. The first one (insertion mechanism *via* H atom migration) involves passage through the H_2O_2 minimum. This pathway can be described as follows: $O(^1D)+H_2O \rightarrow \min 1 \rightarrow ts9 \rightarrow H_2O_2 \rightarrow ts2 \rightarrow \min 2 \rightarrow OH+OH$. Saddle point ts9 leads to the formation of H_2O_2 from min 1 and the second saddle point (ts2) connects the hydrogen peroxide molecule with min 2. The open-shell singlet character is clear for $O(^1D)+H_2O$ and disappears when min 1 is formed. ts9 and H_2O_2 are also closed-shell singlets, but the open-shell character appears again when the hydrogen peroxide dissociates to give OH+OH.

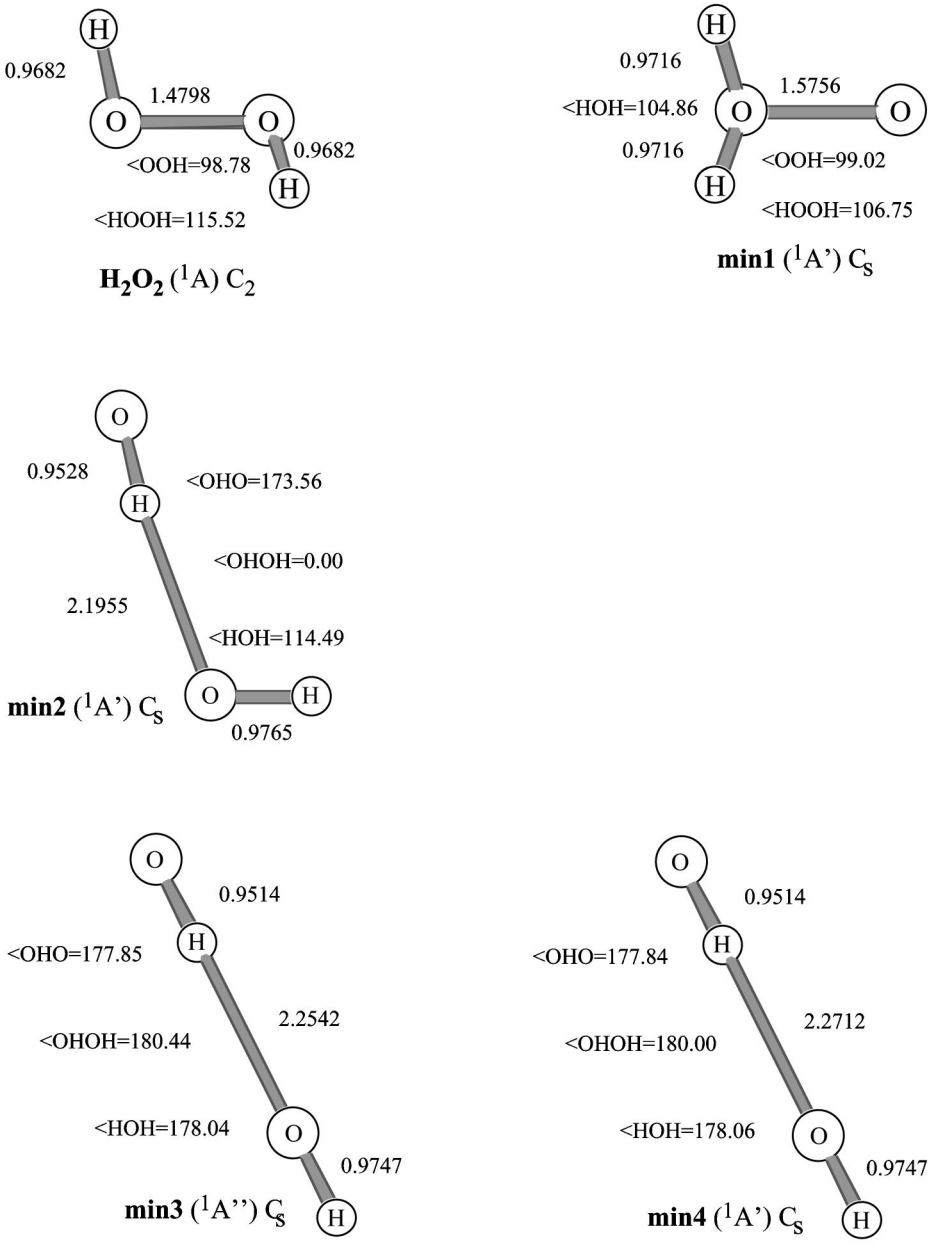

FIG. 2. Minima of the ground PES at the CASSCF(14,10)/cc-pVTZ level of calculation. Distances are in Angstrom and angles are in degrees.

This reaction path was described in our Møller–Plesset study,[22] in which a saddle point (ts8) responsible for the formation of min 1 from reactants was also reported. However, as indicated in that work, ts8 stabilizes below reactants at the highest level of calculation considered [PUMP4(FU)//UMP2(FC)/6-311G($3d2f$,$3p2d$) method]. Here, the CASSCF calculations enabled us to verify that reactants can connect with min 1 without surmounting any energy barrier. To obtain additional confirmation of this barrierless connection we carried out a relaxed scan calculation in C_S symmetry, where the approaching distance between the two oxygen atoms was varied from 2.6 to 1.6 Å. The energies calculated were always placed below the reactants energy, and the energy gradient with respect to the OO distance did not present a change of sign within the range of distances explored. This last result means that at the CASSCF level there are no stationary points between reactants and min 1. The structures of min 1 and ts9 obtained here are very close to those obtained in Ref. 22. This may be explained on the basis of the closed-shell singlet character of both structures. In addition, the vibration mode of ts9 with imaginary frequency ($1268.95i$ cm^{-1}) describes the migration of a hydrogen atom from one oxygen atom to the other one to produce H_2O_2.

In the MP study,[22] ts2 stabilizes below products at the highest level of calculation employed. This was also observed at the CASSCF level, but in this case a minimum (min 2) was located between ts2 and products. The CASSCF geometry found here for ts2 differs from that previously obtained.[22] The main reason for this may be that the electronic structure of this saddle point corresponds to an open-shell singlet. The CASSCF structure is consistently more like the MRCI–SD (multireference configuration interaction method including single and double excitations) structure de-

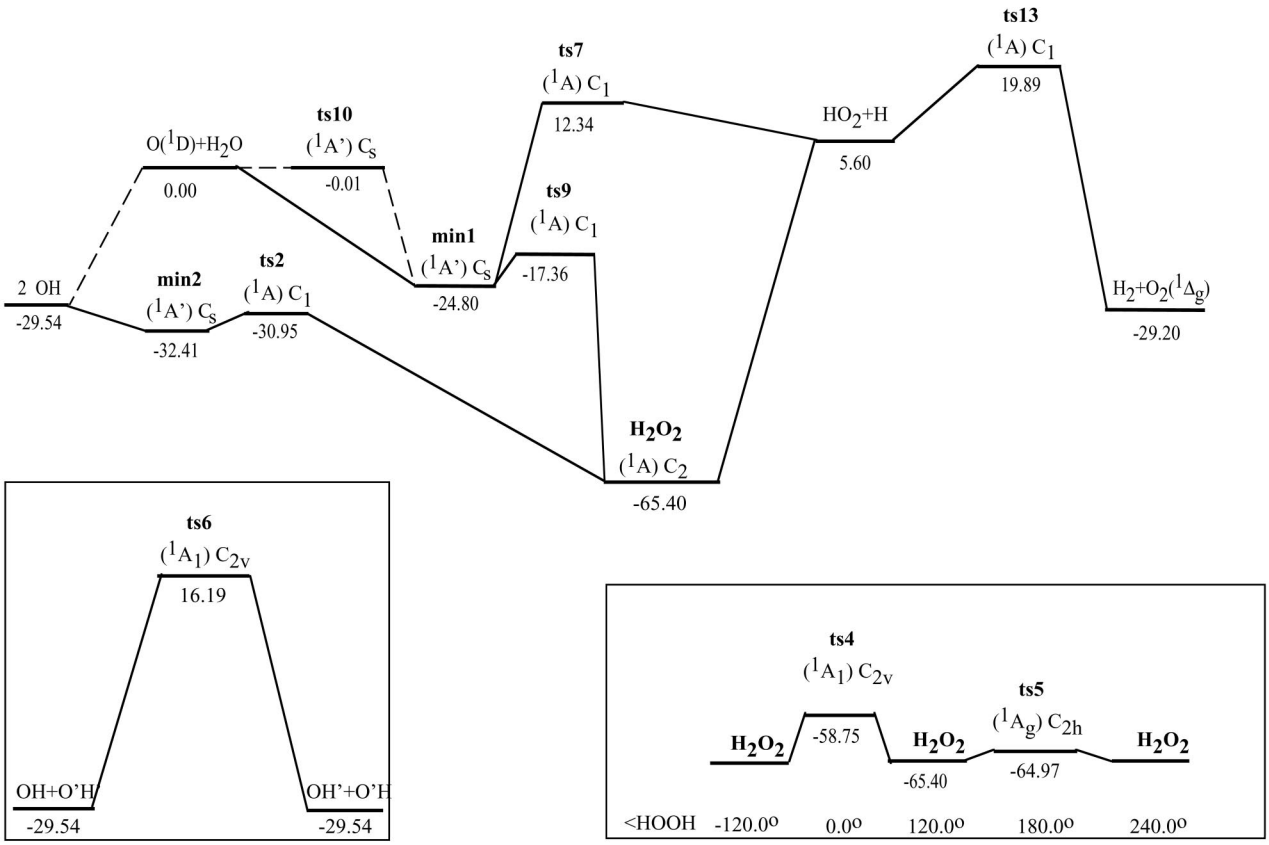

FIG. 3. Energy diagram of the ground PES at the CASSCF(14,10)/cc-pVTZ level of calculation. The energy values include the ZPE and are given from reactants (in kcal mol^{-1}).

scribed in Ref. 21. For ts2 the largest difference is found in the case of the <(HOOH) dihedral angle [143° (MRCI–SD),[21] 131.1° (CASSCF, present study) and 180.0° (UMP2)[22]]. Other OH+OH long-range structures somewhat similar to min 2 were also found: min 3, min 4, ts12, and ts14. These structures and other similar ones were also obtained at the MRCI–SD level.[21] The OH+OH long-range stationary points were not located at the UMP2 level,[22] as there were convergence problems.

A minimum energy path (MEP) calculation to examine further the accuracy of our previous Møller–Plesset calculations[22] was considered. A scan was performed for the $H_2O_2 \rightarrow OH+OH$ dissociation, so varying the OO distance. Results are shown in Fig. 5, where we compare the present CASSCF and CASPT2//CASSCF calculations with our previous PUMP4//UMP2 data, which were used to derive a pseudotriatomic $[O(^1D)+H(OH)]$ analytical potential energy surface for this system.[22] The results are similar to those obtained at the PUMP4//UMP2 level, but significant geometry and energy differences appear. The largest difference between the CASSCF and UMP2 geometries involves the dihedral angle. For the UMP2 scan the <HOOH dihedral angle has a value of 120–130° for OO distances within the range 1.5–2.0 Å, and a value of 180° for larger distances. For the CASSCF calculation <HOOH increases progressively with the OO distance, and reaches 180° only for distances equal to or larger than 3.0 Å.

At the MP level it was found[22] that reaction (1) could also occur through a second reaction pathway (abstraction mechanism). The abstraction of an H atom of the H_2O molecule by the attacking $O(^1D)$ atom to give two OH radicals took place through the saddle point ts10. Here, the CASSCF saddle point ts10 (open-shell singlet with the following main configurations: $6a'^2 7a'^2 8a'^1 1a''^2 2a''^0$ and $6a'^2 7a'^2 8a'^0 1a''^2 2a''^2$ with CI coefficients of 0.70 and −0.70, respectively) is very different from the MP one, being closer in geometry and energy to reactants. This may be due to the large spin contamination present in the previously reported UMP2 structure. In fact, additional calculations carried out on the $O(^3P)+H_2O$ system allowed us to verify that the UMP2 geometry for ts10 is very close to the triplet geometry, which corresponds to the abstraction mechanism on the $^3A''$ PES. It is not completely clear that this saddle point connects reactants with OH+OH, since it exhibits an energy a little below reactants. In fact, we were not able to complete an IRC calculation and, in addition, the vibration mode with imaginary frequency corresponded to an out-of-plane movement. Thus, this saddle point could connect reactants with min 1 through an out-of-plane movement that would allow the attacking $O(^1D)$ atom to approach the water oxygen atom, and the abstraction process could take place without involving a saddle point.

The absence of an energy barrier above reactants along the minimum energy path of reaction (1), predicted by the *ab initio* calculations, is consistent with the fact that, within the temperature range for which the experimental data are avail-

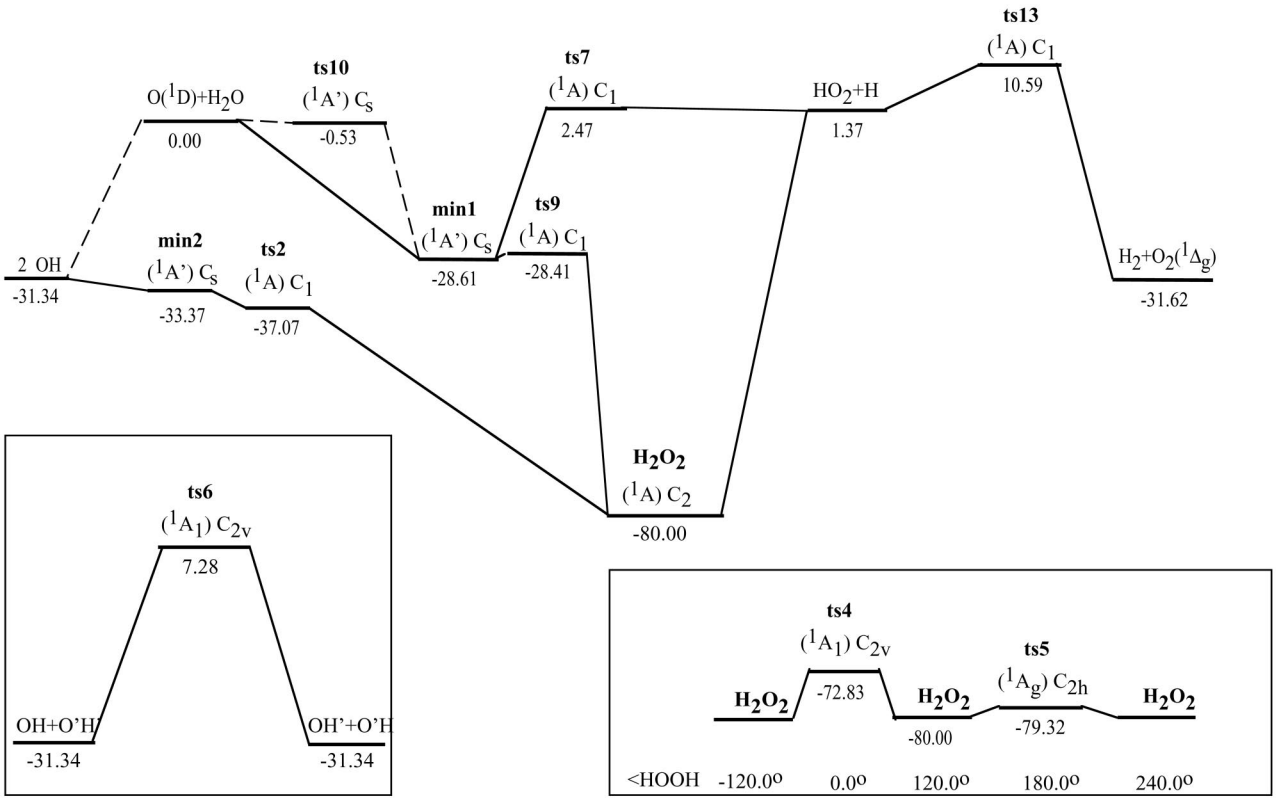

FIG. 4. Energy diagram of the ground PES at the CASPT2(G2)//CASSCF(14,10)/cc-pVTZ level of calculation. The energy values include the CASSCF(14,10)/cc-pVTZ ZPE and are given from reactants (in kcal mol^{-1}).

able ($T=200-350$ K), the rate constant is independent of the temperature (absence of experimental activation energy).[4]

The isomerization of H_2O_2 through ts9 to give min 1 was previously described in the context of a CCSD(T) *ab initio* study (coupled cluster approach including single and double excitations (CCSD) with connected triple excitations).[19] In that work TZ2P+f and DZP basis sets were used for geometry optimizations and harmonic vibrational frequency calculations. However, for the harmonic frequency calculations of ts9 and H_2O_2 the CCSD method was employed instead of the CCSD(T) one. The geometry and harmonic frequencies of min 1, ts9, and H_2O_2 reported here are quite similar to those given in Ref. 19. Nevertheless, the barrier for isomerization from min 1 to H_2O_2 obtained here (0.20 kcal mol^{-1}) differs from those reported in Refs. 19 and 22 (PUMP4//UMP2) (3.2 and 2.83 kcal mol^{-1}, respectively).

For reaction (2) only a stationary point (ts11) with two

TABLE III. Harmonic vibrational frequencies (in cm^{-1}) of the stationary points at the CASSCF(14,10)/cc-pVTZ level.[a]

Mode	ts2 C_1	ts3 C_s	ts4 C_{2v}	ts5 C_{2h}	ts6 C_{2v}	ts7 C_1	ts9 C_1	ts10 C_s
ω_1	3661.16 (A)	1395.90 (A'')	3725.59 (A_1)	3753.94 (B_u)	2356.87 (A_1)	3530.51 (A)	3728.22 (A)	3874.22 (A')
ω_2	3681.17 (A)	1268.71 (A'')	3688.98 (B_2)	3743.09 (A_g)	1547.33 (A_1)	1365.92 (A)	2888.24 (A)	3761.16 (A')
ω_3	312.26 (A)	1149.87 (A'')	1448.53 (B_2)	1522.34 (A_g)	1060.39 (B_2)	1037.57 (A)	1490.78 (A)	1716.00 (A'')
ω_4	193.05 (A)	398.42 (A'')	1343.79 (A_1)	1236.66 (B_u)	960.52 (A_1)	925.11 (A)	936.24 (A)	553.84 (A'')
ω_5	94.86 (A)	518.25i (A'')	827.57 (A_1)	841.29 (A_g)	604.14i (A_1)	752.41 (A)	692.63 (A)	68.04 (A')
ω_6	252.01i (A)	3647.97i (A')	563.28i (A_2)	258.06i (A_u)	2293.27i (B_2)	1068.91i (A)	1268.95i (A)	431.23i (A'')

Mode	ts11 C_s	ts12 C_{2h}	ts13 C_1	ts14 C_s	min 1 C_s	min 2 C_s	min 3 C_s	min 4 C_s	[b]
ω_1	1932.19 (A')	3656.52 (B_u)	1630.82 (A)	4057.64	3780.86 (A'')	4023.40 (A')	4058.41	4056.19	$strOH_1$–$strOH_2$
ω_2	1192.66 (A'')	3653.66 (A_g)	1306.01 (A)	3704.82	3689.29 (A')	3689.56 (A')	3717.38	3717.40	$strOH_2$
ω_3	1050.57 (A')	434.14 (A_g)	1163.83 (A)	300.39	1683.12 (A')	387.87 (A'')	347.89	315.40	*cis*–bend
ω_4	965.19 (A')	176.40 (A_u)	587.68 (A)	93.08	886.05 (A')	378.55 (A'')	134.72	133.23	*trans*–bend
ω_5	1485.83i (A'')	114.06 (A_g)	415.13 (A)	131.34i	876.97 (A'')	177.12 (A')	107.91	104.93	$strOH_3$
ω_6	1939.27i (A')	157.33i (B_u)	3252.87i (A)		674.69 (A')	128.41 (A')			

[a]The vibrational frequencies have been calculated using C_1 symmetry in all cases, except for ts14, min 3, and min 4. For these structures the calculations at this symmetry were not possible due to CASSCF convergence problems. Because of this the frequencies of the out-of-plane vibrational modes of these stationary points were not obtained.

[b]For ts14, min 3, and min 4, $strOH_1$ and $strOH_3$ correspond to the shorter and longer OH bonds, respectively.

TABLE IV. Electronic configurations of the main stationary points at the CASSCF(14,10) level.[a]

Reaction channel (1)	
$O(^1D)+H_2O$	$6a^27a^28a^29a^210a^0(0.68)/6a^27a^28a^29a^0 10a^2(-0.68)$
min 1 (C_s)	$6a'^27a'^21a''^22a''^2(0.98)$
ts9 (C_1)	$6a^27a^28a^29a^2(0.97)$
$H_2O_2(C_2)$	$4a^25a^23b^24b^2(0.97)$
ts2 (C_1)	$6a^27a^28a^29a^210a^0(0.73)/6a^27a^08a^29a^210a^2(-0.66)$
min 2 (C_s)	$6a'^27a'^28a'^21a''^22a''^0(0.71)/6a'^27a'^28a'^21a''^02a''^2(-0.69)$
OH+OH	$6a^27a^28a^29a^210a^0(0.67)/6a^27a^28a^29a^0 10a^2(-0.67)$
Reaction channel (2)	
$O(^1D)+H_2O$	$6a^27a^28a^29a^210a^0(0.68)/6a^27a^28a^29a^0 10a^2(-0.68)$
min 1 (C_s)	$6a'^27a'^21a''^22a''^2(0.98)$
ts11 (C_s)[b]	$6a'^27a'^21a''^22a''^2(0.94)$
$H_2+O_2(a\,^1\Delta_g)$	$6a^27a^28a^29a^210a^0(0.67)/6a^27a^28a^29a^0 10a^2(-0.67)$
Reaction channel (3)[c]	
$O(^1D)+H_2O$	$6a^27a^28a^29a^210a^0(0.68)/6a^27a^28a^29a^0 10a^2(-0.68)$
min 1 (C_s)	$6a'^27a'^21a''^22a''^2(0.98)$
ts7 (C_1)	$6a^27a^28a^29a^210a^0(0.89)/6a^27a^28a^29a^0 10a^2(-0.38)$
$H+HO_2$	$6a^27a^28a^29a^210a^0(0.67)/6a^27a^28a^29a^0 10a^2(-0.67)$

[a]For each stationary point the leading configurations and CI coefficients (in parentheses) are given.
[b]Second order saddle point.
[c]For this channel the following reaction path is also possible: $O(^1D)+H_2O\rightarrow$min 1$\rightarrow$ts9$\rightarrow H_2O_2\rightarrow H+HO_2$.

imaginary frequencies (second-order saddle point) that connects min 1 with the $H_2+O_2(a\,^1\Delta_g)$ products was found. This stationary point has closed-shell character, with the same dominant electronic configuration as min 1 (CI coefficient of 0.94), and is quite similar to the previous one reported by us at the UMP2 level.[22] The difficulties in determining the true (first-order) saddle point are probably because in this case, in order to evolve from reactants to products, two bonds should be formed and two bonds should be broken. This should involve a significant energy barrier from reactants. The energy associated with ts11 (21.5 kcal mol^{-1}) is consistent with this fact and is significantly smaller than the PUMP4//UMP2 energy (28.3 kcal mol^{-1}).[22] Of course, the energy of the true saddle point must be lower than this value. We characterized the vibration modes of ts11 for both imaginary frequencies. The one for $\omega=1939.27i$ cm^{-1} corresponds to a concerted breakage of both OH bonds and the formation of the HH bond, while the one for $\omega=1485.83i$ cm^{-1} corresponds to an antisymmetric motion of both OH bonds.

When we try to remove either the first or the second imaginary modes, we obtain ts13 in both cases. This is a new structure not found in our Møller–Plesset study[22] and is related to ts3. This last saddle point, also described in our previous paper, connects $H_2+O_2(a\,^1\Delta_g)$ with the products of reaction (3) ($H+HO_2$), and has an energy of 12.52 kcal mol^{-1} (2.25 kcal mol^{-1} above $H+HO_2$).[22] At the CASSCF level, ts3 is quite similar to its counterpart already described in Ref. 22, but it has two imaginary frequencies ($3647.97i$ and $518.25i$ cm^{-1}). The former is associated to the breaking of the OH bond and the formation of the HH bond, and the latter corresponds to an out-of-plane motion. After removing the last frequency, we obtained ts13 again, whose imaginary vibration frequency corresponds to the first motion previously described for ts3. The connectivity of ts13 was studied by means of an IRC calculation, which confirmed that the reaction $H+HO_2\rightarrow H_2+O_2(a\,^1\Delta_g)$ proceeds through ts13. This saddle point has an energy of 10.59 kcal mol^{-1} (9.22 kcal mol^{-1} above $H+HO_2$). Reactants ($H+HO_2$), products [$H_2+O_2(a\,^1\Delta_g)$] and saddle point (ts13) are open-shell singlets.

The production of atomic hydrogen and hydroperoxy radical [reaction (3)] can also take place *via* two possible reaction pathways, as in the case of reaction (1). The first pathway (insertion mechanism *via* H atom migration), analogous to the one for reaction (1), involves the H_2O_2 hydrogen peroxide minimum [$O(^1D)+H_2O\rightarrow$min 1$\rightarrow$ts9$\rightarrow H_2O_2\rightarrow H+HO_2$]. Thus, this reaction path is identical to that for reaction (1) up to the H_2O_2 minimum. We could not reproduce the saddle point ts1 previously described in Ref. 22 (UMP2 level), which was situated in the exit channel. Thus, the connection between the hydrogen peroxide molecule and products takes place without any energy barrier.

As for reaction (1), a MEP calculation was considered to compare with our previous Møller–Plesset calculations.[22] A scan starting at the H_2O_2 molecule and running up to the $H+HO_2$ product asymptote was performed, varying one of the OH distances (Fig. 5). For the $H_2O_2\rightarrow H+HO_2$ dissociation, the geometries at both levels of calculation (CASSCF and UMP2) are quite close to each other, but important energy differences appear in the CASSCF, CASPT2//CASSCF, and PUMP4//UMP2 MEP calculations.

Reaction (3) can also occur through a second pathway (substitution mechanism). A saddle point (ts7) bearing an open-shell singlet character and describing the evolution from min 1 to the hydroperoxy radical was found, with an energy of 2.47 kcal mol^{-1}. This saddle point is slightly different from the UMP2 one.[22] The imaginary vibration mode of ts7 ($\omega=1068.91i$ cm^{-1}) corresponds to the stretching motion of the longer OH bond (1.5627 Å).

A MEP was constructed to verify the connectivity be-

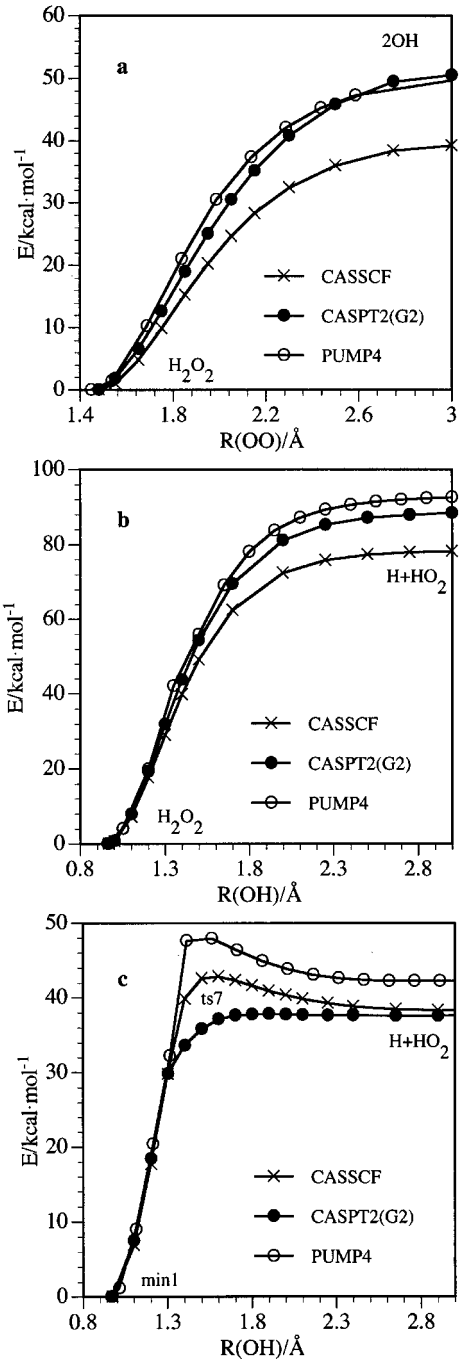

FIG. 5. Minimum energy paths using different *ab initio* methods for (a) $H_2O_2 \rightarrow 2OH$; (b) $H_2O_2 \rightarrow H+HO_2$; (c) min 1$\rightarrow$ts7$\rightarrow H+HO_2$. The PUMP4 results correspond to the highest level of calculation of Ref. 22. The CASPT2 and PUMP4 methods correspond to the CASPT2//CASSCF and PUMP4//UMP2 levels of calculation, respectively (see text).

tween min 1, ts7, and $H+HO_2$ (Fig. 5), and was compared with our previous PUMP4//UMP2 results.[22] In this case, the CASSCF and UMP2 geometries are quite close to each other, but the CASPT2//CASSCF and PUMP4//UMP2 energies are quite different. ts7 was placed 1.10 kcal mol^{-1} above $H+HO_2$ at the CASPT2//CASSCF level, while at the PUMP4//UMP2 level a value of 5.43 kcal mol^{-1} was obtained.

Figures 3 and 4 also include other saddle points (ts4 and ts5) which are associated to the internal rotation of the hydrogen peroxide molecule. They are closed-shell species, their electronic configuration being $6a'^2 7a'^2 1a''^2 2a''^2$ with a coefficient of 0.97 in both cases. ts4 presents a dihedral angle of 0° (*cis*-arrangement) while ts5 presents a dihedral angle of 180° (*trans*-arrangement). Saddle point ts4 is more energetic than ts5 because two different repulsive interactions are possible in the *cis*-geometry: one between the oxygen lone pair electrons and one between the OH bond dipole moments. In the *trans*-geometry (ts5) only the first repulsive interaction is possible. The calculated barriers for the internal rotation of H_2O_2 are 7.59 kcal mol^{-1} (*cis*) and 1.01 kcal mol^{-1} (*trans*), both without including the ZPE. These values compare very well with the experimental data [7.11 kcal mol^{-1} (*cis*) and 1.10 kcal mol^{-1} (*trans*),[37] 7.33 kcal mol^{-1} (*cis*) and 1.11 kcal mol^{-1} (*trans*)[38]] and with the highest level Møller–Plesset values reported by us[22] [7.38 kcal mol^{-1} (*cis*) and 1.23 kcal mol^{-1} (*trans*)].

The saddle point for the exchange process of the hydrogen atoms between the two hydroxyl radicals (ts6) was also found. ts6 is an open-shell singlet with the following main configurations: $6a'^2 7a'^0 8a'^2 1a''^2 2a''^2$ and $6a'^0 7a'^2 8a'^2 1a''^2 2a''^2$ with CI coefficients of 0.81 and -0.54, respectively. It is a highly symmetric and energetic saddle point, as it was at the UMP2 level.[22] However, at the CASSCF level this stationary point has two imaginary vibration modes ($\omega = 2293.27i$ and $604.14i$ cm^{-1}) and is not a planar structure, which is at variance with the UMP2 calculation.[22]

IV. SUMMARY AND CONCLUSIONS

The ground potential energy surface of the $O(^1D)+H_2O$ system was studied employing the CASPT2//CASSCF *ab initio* method and using the cc-pVTZ basis set for most of the calculations. Reactants, products, and the saddle points and minima (one of them corresponding to the hydrogen peroxide molecule) placed between them were characterized. This study sought to analyze the degree of validity of an earlier *ab initio* study by us[22] using the Møller–Plesset method, because the previously obtained UMP2 geometries for open-shell singlet stationary points could be placed between the hypothetical correct singlet and triplet ones, due to spin contamination.

Both the present CASPT2//CASSCF calculations and the highest level Møller–Plesset calculations (PUMP4//UMP2) previously reported show that the main reaction channel (OH +OH) has no energy barrier along the minimum energy path (insertion *via* H atom migration leading to H_2O_2 and then to products). This result is consistent with the absence of experimental activation energy. In addition, the geometry of those stationary points bearing an open-shell singlet character does not depend much on the level of calculation, be it CASSCF or UMP2. The exception is ts10, which is substantially closer (in geometry and energy) to reactants at the CASSCF level.

In spite of the above-mentioned results, the CASPT2//CASSCF and PUMP4//UMP2 results show considerable differences, particularly in the energy, due to the dominant open-shell singlet character of the ground potential energy surface. The $H_2O_2 \rightarrow 2$ OH minimum energy path involved in

the insertion mechanism of reaction (1) is described in a similar way at the CASPT2//CASSCF and PUMP4//UMP2 levels. However, significant geometry and energy differences exist. The CASPT2//CASSCF min $1 \rightarrow H_2O_2$ isomerization barrier involved in this mechanism is considerably smaller (0.20 kcal mol^{-1} above min 1) than the PUMP4//UMP2 one (2.83 kcal mol^{-1} above min 1). Besides, the OH+OH long-range stationary points were not found at the Møller–Plesset level due to UMP2 convergence problems. In addition, the highly energetic PUMP4//UMP2 saddle point for the abstraction mechanism of reaction (1) was not found at the CASPT2//CASSCF level.

In reaction (2), the CASPT2//CASSCF energy (21.5 kcal mol^{-1} above products) associated to the second-order saddle point determined is substantially smaller than the PUMP4//UMP2 energy (28.3 kcal mol^{-1} above products). For the $H_2O_2 \rightarrow H+HO_2$ MEP describing the insertion mechanism of reaction (3), important differences arise for the energy when comparing the CASPT2//CASSCF and PUMP4//UMP2 results. Moreover, the saddle point for the substitution mechanism arising from min 1 has a substantially smaller energy in the CASPT2//CASSCF case (1.10 kcal mol^{-1} above products) than in the PUMP4//UMP2 one (5.40 kcal mol^{-1} above products).

In conclusion, an accurate general description of the $O(^1D)+H_2O$ system, particularly regarding the energetics, requires *ab initio* calculations using multireference methods such as the method considered here. Nevertheless, the previous highest level Møller–Plesset calculations (PUMP4//UMP2)[22] can be taken as a reasonable starting point for characterizing the ground PES of the system. In addition, the pseudotriatomic $[O(^1D)+H-(OH)]$ analytical potential energy surface derived in the previous study to help interpret the experimental results can be considered quite reasonable for modeling the $O(^1D)+H_2O \rightarrow 2\,OH$ reaction, as the large PUMP4//UMP2 energy barrier found there for the abstraction mechanism was not included in the fit.

The values of the coefficients of the polynomial involved in the triatomic analytical PES reported by us in Ref. 22 (Table III) should be multiplied by the value of the C000 coefficient to obtain the correct values, with the exception of this last coefficient that was already correct.

ACKNOWLEDGMENTS

This study was supported by the ''Dirección General de Enseñanza Superior'' of the Spanish Ministry of Education and Culture through the DGES project PB98-1209-C02-01. C.O. thanks the Spanish Ministry of Education and Culture for a predoctoral research grant. The authors are also grateful to the ''Generalitat de Catalunya'' (Autonomous Government of Catalonia) for partial support (Refs. 1998SGR 00008 and 2000SGR 00016), and to the ''Center de Supercomputació i Comunicacions de Catalunya (C^4–CESCA/CEPBA)'' for computer time made available.

[1] J. R. Wiesenfeld, Acc. Chem. Res. **15**, 110 (1982).
[2] P. Warneck, *Chemistry of the Natural Atmosphere* (Academic, San Diego, 1988).
[3] M. W. Chase, Jr., C. A. Davies, J. R. Downey, Jr., D. J. Frurip, R. A. McDonald, and A. N. Syverud, J. Phys. Chem. Ref. Data Suppl. **14**, 1 (1985).
[4] R. Atkinson, D. L. Baulch, R. A. Cox, R. F. Hampson, Jr., J. A. Kerr, and J. Troe, J. Phys. Chem. Ref. Data **21**, 1125 (1992).
[5] R. Zellner, G. Wagner, and B. Himme, J. Phys. Chem. **84**, 3196 (1980).
[6] J. E. Butler, L. D. Talley, G. K. Smith, and M. C. Lin, J. Chem. Phys. **74**, 4501 (1981).
[7] K.-H. Gericke, F. J. Comes, and R. D. Levine, J. Chem. Phys. **74**, 6106 (1981).
[8] F. J. Comes, K.-H. Gericke, and J. Manz, J. Chem. Phys. **75**, 2853 (1981).
[9] W. A. Guillory, K.-H. Gericke, and F. J. Comes, J. Chem. Phys. **78**, 5993 (1983).
[10] C. B. Cleveland and J. R. Wiesenfeld, J. Chem. Phys. **96**, 248 (1992).
[11] D. G. Sauder, J. C. Stephenson, D. S. King, and M. P. Casassa, J. Chem. Phys. **97**, 952 (1992).
[12] D. S. King, D. G. Sauder, and M. P. Casassa, J. Chem. Phys. **97**, 5919 (1992).
[13] D. S. King, D. G. Sauder, and M. P. Casassa, J. Chem. Phys. **100**, 4200 (1994).
[14] N. Tanaka, M. Takayanagi, and I. Hanazaki, Chem. Phys. Lett. **254**, 40 (1996).
[15] N. Tanaka, U. Nagashima, M. Takayanagi, H. L. Kim, and I. Hanazaki, J. Phys. Chem. A **101**, 507 (1997).
[16] H. Tsurumaki, Y. Fujimura, and O. Kajimoto, J. Chem. Phys. **110**, 7707 (1999).
[17] K. Imura, M. Veneziani, T. Kasai, and R. Naaman, J. Chem. Phys. **111**, 4025 (1999).
[18] L. B. Harding, J. Phys. Chem. **93**, 8004 (1989).
[19] C. Meredith, T. P. Hamilton, and H. F. Schaefer III, J. Phys. Chem. **96**, 9250 (1992).
[20] J. Koput, S. Carter, and N. C. Handy, J. Phys. Chem. A **102**, 6325 (1998).
[21] L. B. Harding, J. Phys. Chem. **95**, 8653 (1991).
[22] R. Sayós, C. Oliva, and M. González, J. Chem. Phys. **113**, 6736 (2000).
[23] R. Sayós, C. Oliva, and M. González, in *Reaction and Molecular Dynamics*, Lecture Notes in Chemistry, Vol. 75, edited by A. Laganà and A. Riganelli (Springer, Berlin, 2000), p. 279.
[24] MOLCAS 4.1 program, K. Andersson, M. R. A. Blomberg, M. P. Fülscher *et al.*, Lund University, Sweden, 1998.
[25] GAMESS 96 program, M. W. Schmidt, K. K. Baldridge, J. A. Boatz *et al.* [J. Comput. Chem. **14**, 1347 (1993)].
[26] K. Andersson, P.-A. Malmqvist, and B. O. Roos, J. Chem. Phys. **96**, 1218 (1992).
[27] Landolt-Börnstein, in *Structure Data of Free Polyatomic Molecules*, edited by W. Martienssen (Springer-Verlag, Berlin, 1998), Vol. II/25A.
[28] W. B. Olson, R. H. Hunt, B. W. Young, A. G. Maki, and J. W. Brault, J. Mol. Spectrosc. **127**, 12 (1988).
[29] W. B. Cook, R. H. Hunt, W. N. Shelton, and F. A. Flaherty, J. Mol. Spectrosc. **171**, 91 (1995).
[30] A. Perrin, A. Valentin, J.-M. Flaud, C. Camy-Peyret, L. Schriver, A. Schriver, and Ph. Arcas, J. Mol. Spectrosc. **171**, 358 (1995).
[31] C. Camy-Peyret, J.-M. Flaud, J. W. C. Johns, and M. Nöel, J. Mol. Spectrosc. **155**, 84 (1992).
[32] T. Shimanouchi, J. Phys. Chem. Ref. Data **6**, 993 (1977).
[33] S. Bashkin and J. O. Stoner, *Atomic Energy Levels and Grotrian Diagrams* (North-Holland, Amsterdam, 1975), Vol. 1.
[34] K. P. Huber and G. Herzberg, *Molecular Spectra and Molecular Structure* (Van Nostrand Reinhold, New York, 1979), Vol. 4.
[35] G. Herzberg, *Molecular Spectra and Molecular Structure* (Van Nostrand Reinhold, New York, 1966), Vol. 3.
[36] W. E. Thompson and M. E. Jacox, J. Chem. Phys. **91**, 3826 (1989).
[37] J. Koput, J. Mol. Spectrosc. **115**, 438 (1986).
[38] J.-M. Flaud, C. Camy-Peyret, J. W. C. Johns, and B. Carli, J. Chem. Phys. **91**, 1504 (1989).